Bull. Chem. Soc. Jpn., 71, 1241—1248 (1998)

Dynamic Stereochemistry of *N*-Phenyl-9-triptycylamine and Its *N*-Alkyl Derivatives[#]

Gaku Yamamoto,* Katsuya Inoue, Hiroyuki Higuchi,[†] Masami Yonebayashi,[†] Yuki Nabeta,[†] and Jūro Ojima[†]

Department of Chemistry, School of Science, Kitasato University, Sagamihara, Kanagawa 228

†Department of Chemistry, Faculty of Science, Toyama University, Gofuku, Toyama 930

(Received January 7, 1998)

In *N*-phenyl-9-triptycylamine (**6**), "gear rotation" (GR) and "isolated rotation" (IR) have almost the same free-energy barriers of ca. 45.2 kJ mol^{-1}, while the nitrogen inversion is fast throughout the whole temperature range and thus the nitrogen is regarded as planar on the NMR timescale. In *N*-methyl-*N*-phenyl-9-triptycylamine (**7**), the internal motions are fast on the NMR time scale even at the lowest attainable temperature. In *N*-benzyl-*N*-phenyl-9-triptycylamine (**8**), the GR process has a free-energy barrier of ca. 36 kJ mol^{-1} and the passing of the benzyl group over an *o*-benzeno group has a higher barrier than GR. *N*-2-Biphenylyl-9-triptycylamine (**9**), which is obtained during the course of the synthesis of **6**, shows a dynamic behavior presumably ascribable to GR with the free-energy barrier of 70 kJ mol^{-1}.

Correlated internal rotation in molecules containing aromatic rings has long been a subject of interest. Molecular propellers, Ar_nX where aryl (Ar) groups bond to a central atom X,[1] and molecular gears, Tp_2X[2] and ArXTp[3] where Tp denotes a 9-triptycyl group, have been extensively studied. We have shown that 9-benzyltriptycene (**1**) and 9-phenoxytriptycene (**2**) (Chart 1), typical examples of ArXTp-type compounds, can be regarded as a static bevel gear system composed of a three-toothed wheel and a two-toothed wheel, adopting a conformation approximately represented by the Newman projection **3** (Chart 2). In these compounds, two kinds of dynamic processes are feasible: "gear rotation" and "isolated rotation." Gear rotation (GR) is correlated disrotation of the Tp–X and Ph–X bonds, the transition state of which is represented by **4** (Chart 2). Isolated rotation (IR) is rotation of the Ph–X bond taking place without rotation of the Tp–X bond, the transition state of which is represented by **5** (Chart 2). In compound **2**, the dynamic process with a lower energy barrier was found to be GR, while in compound **1** the lower-energy process was IR.[4] The difference in behavior between **1** and **2** was ascribed to two main factors: C–X bond lengths and valency of X; shorter C–O bonds cause the tighter meshing of the wheels and thus raise the IR barrier in **2**, rendering GR more favorable in **2**, while the tetravalency of carbon raises the GR barrier in **1**, rendering IR more favorable in **1**.[4]

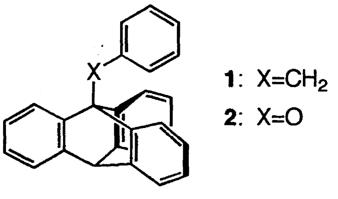

Chart 1.

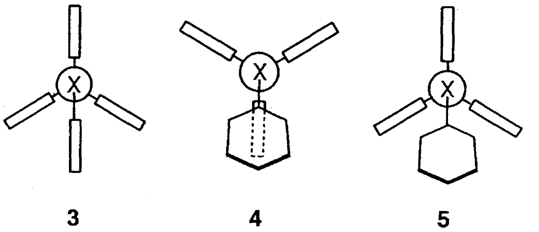

Chart 2.

These findings prompted us to study the dynamic behavior of the corresponding nitrogen analog, *N*-phenyl-9-triptycylamine (**6**). The behavior of **6** is expected to be intermediate between those of **1** and **2**. In addition, another dynamic process, i.e., inversion at the nitrogen atom, may contribute to the total dynamic behavior of the molecule. In this article we report the dynamic stereochemistry of **6**[5] and its *N*-methyl and *N*-benzyl derivatives, **7** and **8**, together with that of *N*-2-biphenylyl-9-triptycylamine (**9**), which was unexpectedly obtained in the course of the synthesis of **6** (Chart 3).

Results and Discussion

Syntheses. *N*-Phenyl-substituted 9-triptycylamines had been a completely unknown group of compounds until we started the investigation. We had established that *N*-alkyl- and *N*,*N*-dialkyl-9-triptycylamines are synthesized by alkylation of 9-triptycylamine which is easily prepared from 9-nitrotriptycene.[6] As it is well-known that benzyne inserts into the N–H bond of a primary amine to give the corresponding *N*-phenyl derivative, we expected that reaction of benzyne

---

[#] Dedicated to Professor Michinori Ōki on the occasion of his 70th birthday.

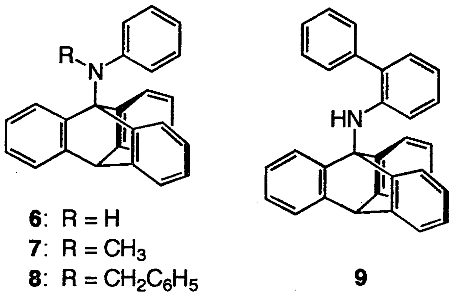

Chart 3.

with 9-triptycylamine would afford *N*-phenyl-9-triptycylamine (**6**). Thus thermal decomposition of benzenediazonium-2-carboxylate was tried in the presence of 9-triptycylamine; this actually afforded the desired product **6** in 46% yield (Scheme 1).

When a large excess amount of benzenediazonium-2-carboxylate was used in this reaction, a second product was obtained at the expense of **6**. The structure of the compound was spectroscopically estimated and finally confirmed by X-ray crystallography to be *N*-2-biphenylyl-9-triptycylamine (**9**) (Fig. 1). Compound **9** should be formed by reaction of benzyne with once formed **6**, because decomposition of benzenediazonium-2-carboxylate in the presence of **6** also affords **9** in a high yield. It is interesting to note that reaction of benzyne with **6** afforded the *C*-phenylated compound **9**, presumably by the ene reaction followed by tautomerization (Scheme 2), instead of the intuitively expected N–H insertion product, *N*,*N*-diphenyl-9-triptycylamine. It may be because the nitrogen in **6** is sterically hindered from the attack of benzyne.

Reaction of butyllithium with **6**, followed by treatment with methyl iodide and benzyl bromide, afforded the corresponding *N*-alkyl derivatives **7** and **8** in 89 and 18% yield, respectively. The low yield of **8** may also be ascribed to steric hindrance.

Dynamic NMR Spectroscopy. Upon examining the stereodynamics of compounds **6**, **7**, and **8**, we can consider three types of dynamic processes: IR and GR processes of the phenyl group and the passing of the remaining nitrogen substituent R over an *o*-benzeno group, which is hereafter referred to as "R-passing". We assume that the nitrogen atom is pyramidal in these compounds, even in compound **6**, since it is well-documented that the nitrogen atom of aniline is pyramidal.[7,8] Two of the dynamic processes, GR and R-passing, are schematically shown as in Scheme 3, where the nitrogen atom is depicted as tetrahedral, although actually the pyramidality would be far shallower especially when R=H. It should be noted that both GR and R-passing involve inversion of the nitrogen atom.

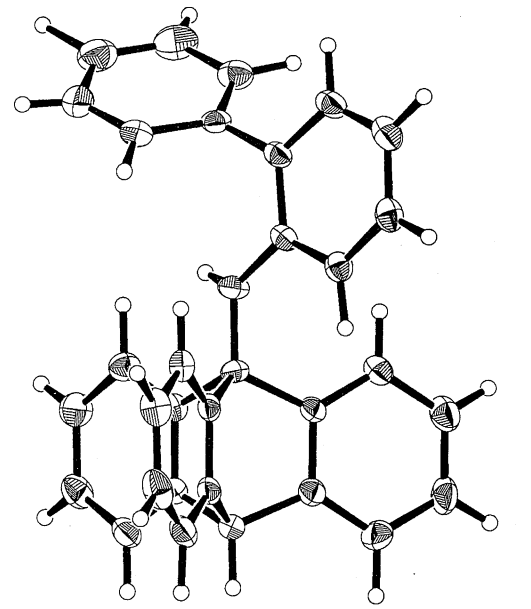

Fig. 1. Molecular structure of *N*-2-biphenylyl-9-triptycylamine (**9**).

The ^{1}H NMR spectra of the *N*-phenyl compound **6** in CD_2Cl_2 at various temperatures are given in Fig. 2. At 26 °C the internal motion is fast on the NMR time scale, though the signal due to the *o*-protons of the phenyl group is broadened. Upon lowering the temperature, all the aromatic proton signals except for the one due to 4′-H broaden, split, and resharpen, indicating that rotations around both the Ph–N and the Tp–N bond slow down. At −87 °C the two edges of the Ph moiety are nonequivalent, and one of the *o*-benzeno rings of the Tp moiety is magnetically different

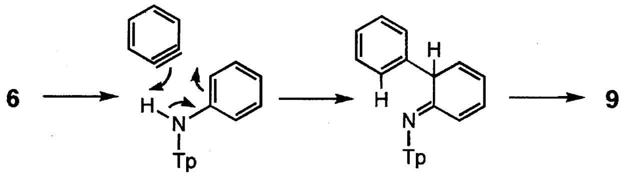

Scheme 2.

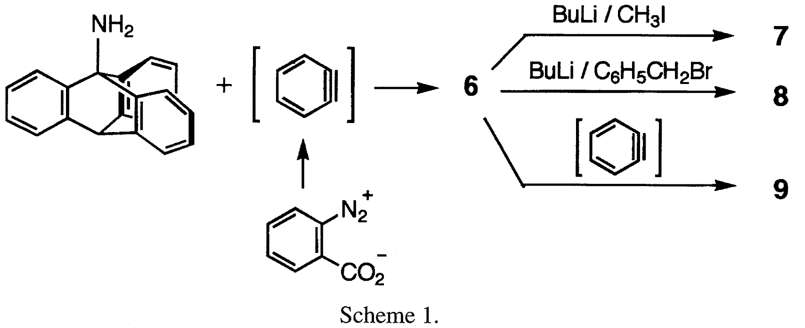

Scheme 1.

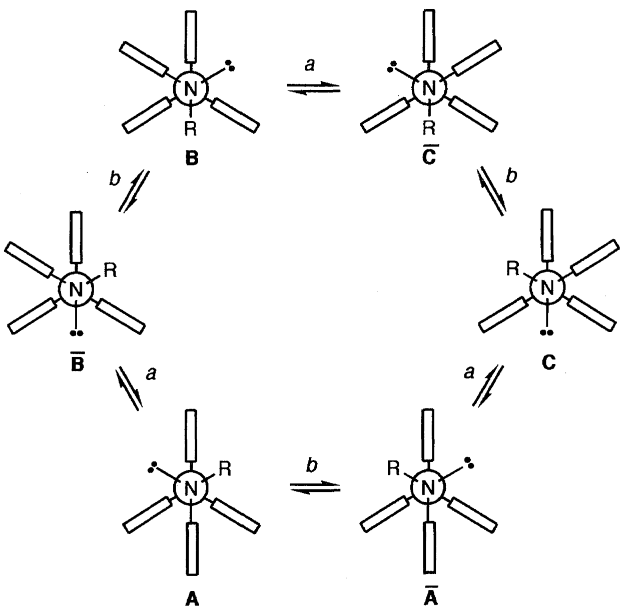

a: "Ph-passing" by GR; b: "R-passing"

Scheme 3.

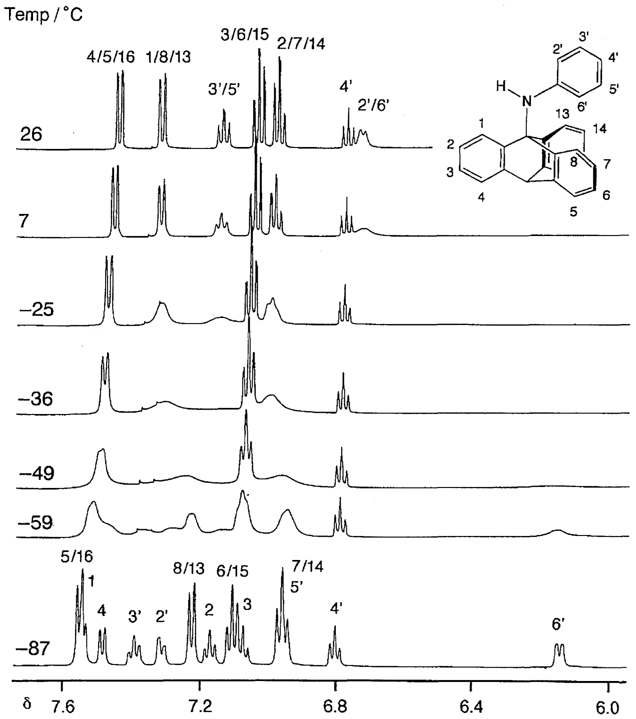

Fig. 2. NMR spectra due to the aromatic protons of *N*-phenyl-9-triptycylamine (**6**) in CD_2Cl_2 at various temperatures.

from the other two.

This situation is more explicitly observed in the ^{13}C NMR spectrum of **6**, the aromatic tertiary carbon region at various temperatures being shown in Fig. 3. At −89 °C the signals due to the *o*- and *m*-carbons of the Ph group appear as two peaks of equal intensity, respectively, while the signals due to the tertiary aromatic carbons of the Tp moiety appear as four pairs of peaks with an intensity ratio of 2 : 1.

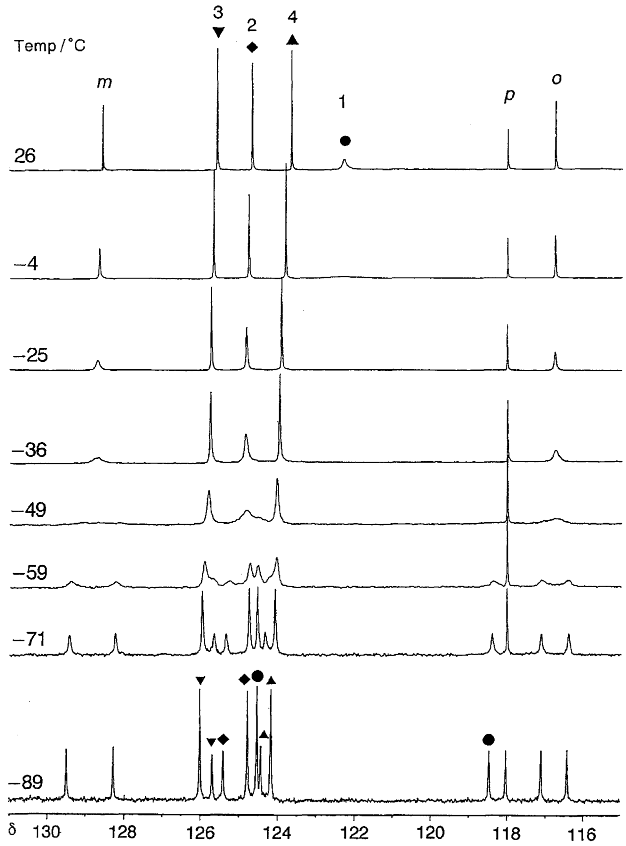

Fig. 3. NMR spectra due to the aromatic tertiary carbons of **6** in CD_2Cl_2 at various temperatures.

At the lowest temperature, therefore, the phenyl group is frozen into a notch made of two *o*-benzeno rings, while the passing of the *N*-hydrogen over an *o*-benzeno group, i.e., "H-passing", is still fast on the NMR time scale.

The lineshape analysis of the *o*- and *m*-carbon signals afforded the free energy of activation of 43.9±0.4 kJ mol^{-1} for the Ph–N rotation in the temperature range from −36 to −71 °C, while the temperature dependence of the 3/6/15-carbon signals afforded 45.2±0.4 kJ mol^{-1} for the Tp–N rotation in this temperature range. Typically the rate constants at −59 °C are found to be 90 and 36 s^{-1} for the Ph–N and the Tp–N rotation, respectively. As discussed in detail before,[4] the Tp–X rotation in a PhXTp compound takes place only by the GR process, while the Ph–X rotation takes place either by GR or by IR. Thus the rate constant for the GR process in **6** is 36 s^{-1} at −59 °C, while that for IR is calculated as $90-36=54$ s^{-1}. This means that the two processes take place at similar rates and thus have almost the same free energy barriers of ca. 45.2 kJ mol^{-1}. Meanwhile the barrier to "H-passing" is estimated to be far lower than 35 kJ mol^{-1}.

In Table 1 are shown the rate constants and the free energies of activation for the GR and IR processes in compounds **1**, **2**, and **6** at −59 °C. The IR rate constant (k_{IR}) monotonously decreases from **1** to **6** to **2** in parallel with the change in the C–X bond length. The shortening of the C–X bonds on going from **1** to **6** to **2** sterically destabilizes both the ground state and the transition state for the IR process. The extent

Table 1. Rate Constants and Free Energies of Activation of the GR and IR Processes in Compounds **1**, **2**, and **6** at −59 °C

Compd	X	k_{GR}	$\Delta G^{\ddagger}_{GR}$	k_{IR}	$\Delta G^{\ddagger}_{IR}$
		s^{-1}	kJ mol^{-1}	s^{-1}	kJ mol^{-1}
1a)	CH_2	52	44.8	2350	38.1
6	NH	36	45.6	54	44.8
2a)	O	ca. 10^5	ca. 29	ca. 10^{-2} b)	ca. 62b)

a) Ref. 4. b) From the molecular mechanics data given in Ref. 4.

of destabilization would be larger in the latter and thus the IR process takes place slower in this order, i.e., $1 > 6 > 2$.

On the contrary, the GR rate constant (k_{GR}) is rather similar in **1** and **6** and significantly increases in **2**. The low GR barrier in **2** has been ascribed to the divalency of the oxygen; the eclipsing interaction at the transition state should be considered only between the phenyl group and one of *o*-benzeno bridges (see **10** in Chart 4) in contrast with the case of **1** where the eclipsing interaction between the methylene hydrogens and the *o*-benzeno bridges should also be considered (see **11**).[4] The bond length effect which would more destabilize **10** than **11** is completely overshadowed by the valency effect.

In the nitrogen compound **6**, the transition state for the GR process would be tentatively represented by **12** with the planar nitrogen atom, because the GR process necessarily involves nitrogen inversion, though the determination of the actual geometry of the transition state requires detailed MO calculations. The similar GR barriers in **1** and **6** will be understood in terms of the destabilization of **12** due to the planar nitrogen together with the bond length effect, which will more destabilize the GR transition state of **6** than that of **1**.

In *N*-methyl-*N*-phenyl-9-triptycylamine (**7**), the change in the NMR lineshape takes place at a far lower temperature range than in the case of **6**. The aromatic proton signals show only extensive broadening even at ca. −100 °C, suggesting that the rate processes occurring in this molecule have significantly low energy barriers of below 30 kJ mol^{-1}. The GR barrier in **7** is expected to be lower than that in **6** because the ground state would be more destabilized in **7** due to larger steric congestion, while the transition-state energy would be similar between **6** and **7**. The passing of the methyl group over an *o*-benzeno group is inferred to have a rather low barrier, judging from the finding that the corresponding barrier is ca. 31.4 kJ mol^{-1} in *N*-ethyl-*N*-methyl-9-triptycylamine, and even lower in *N*,*N*-dimethyl-9-triptycylamine.[6] The IR barrier in **7** may be higher than that in **6**, inferring from the fact that introduction of a methyl group into the methylene moiety of 9-benzyltriptycene raises the IR barrier by ca. 17 kJ mol^{-1} from 38.5 to 55.6 kJ mol^{-1}.[4,9] However, the experimentally observable Ph–N rotation reflects whichever barrier of the GR and IR processes is lower, and thus the IR process would not affect the NMR lineshape of compound **7**.

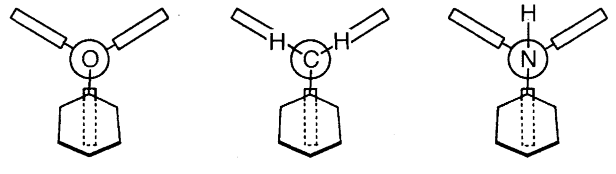

10 **11** **12**

Chart 4.

The ^1H and ^{13}C NMR spectra of *N*-benzyl-*N*-phenyl-9-triptycylamine (**8**) in CD_2Cl_2 show that all the rate processes are fast on the NMR time scale at 24 °C. If one lowers the temperature, both spectra show complex changes; the low-field region of the ^1H spectrum at various temperatures are shown in Fig. 4. The methylene proton signal observed as a singlet at $\delta = 5.44$ at −35 °C decoalesces into an AB-type quartet ($\delta = 5.22$ and 5.67 at −105 °C). The *o*-protons of the *N*-phenyl group affording a broad doublet at $\delta = 6.58$ at −35 °C become diastereotopic: A signal due to one of them appears at $\delta = 5.90$ at −105 °C, while that due to the other one is obscured by other aromatic signals. The *o*-protons of the *C*-phenyl group also become diastereotopic, one of them affording a signal at $\delta = 8.27$ at −105 °C as a broad peak.

Since the complete lineshape analysis was judged to be difficult, the coalescence method was employed to obtain

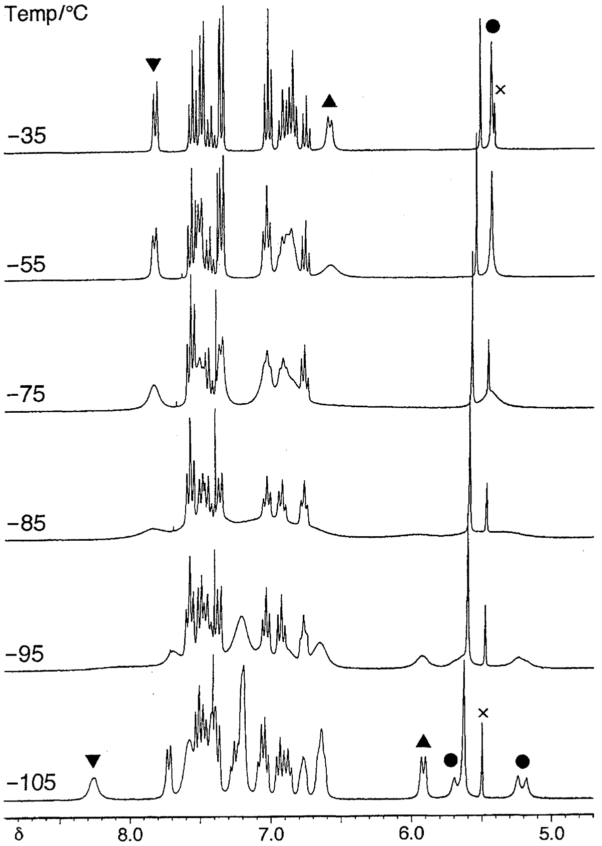

Fig. 4. The low-field region ^1H NMR spectra of *N*-benzyl-*N*-phenyl-9-triptycylamine (**8**) in CD_2Cl_2 at various temperatures. The signals with ● are due to CH_2 and those with ▲ and ▼ are due to the *o*-protons of the *N*-phenyl and *C*-phenyl groups, respectively. The peak with × is due to the solvent.

the approximate rate constants.[10] The rate constant of ca. 300 s^{-1} at ca. -85 °C is deduced from the coalescence of the methylene signal, affording the $\Delta G^{\ddagger}$ value of ca. 36 $kJ\,mol^{-1}$. The coalescence of the *N*-phenyl proton signal gives the rate constant of ca. 800 s^{-1} at ca. -75 °C, corresponding to the $\Delta G^{\ddagger}$ value of ca. 37 $kJ\,mol^{-1}$. Meanwhile the coalescence of the *C*-phenyl proton signal affords the rate constant of ca. 500 s^{-1} at ca. -100 °C, corresponding to the $\Delta G^{\ddagger}$ value of ca. 33 $kJ\,mol^{-1}$. The former two data are best interpreted to reflect the same rate process.

The spectrum at -105 °C (Fig. 4, bottom) indicates that the molecule is frozen into one of the conformers shown in Scheme 3, although the conformation of the benzyl moiety is uncertain. Coalescence of the two signals due to the *o*-protons of the *N*-phenyl group into one upon raising the temperature indicates that either or both of the GR and the IR processes become fast on the NMR timescale. The GR process in compound **8** would have a lower energy barrier than that in **6**, while the IR barrier would be higher in **8** than in **6**, by a similar reasoning to that discussed for **7** previously. Therefore the observed lineshape change is ascribed to the GR process. On the other hand, coalescence of the methylene signal from an AB-type quartet to a singlet indicates that either or both of "Ph-passing" (e.g. $A \rightleftarrows \overline{B}$ in Scheme 3) and "Bzl-passing" (e.g. $A \rightleftarrows \overline{A}$ in Scheme 3) become fast on the NMR timescale, the former taking place with gear rotation (GR). If we assume that the coalescence phenomena observed for the *N*-phenyl and methylene signals reflect the same rate process, the process should be "Ph-passing" or the GR process, the $\Delta G^{\ddagger}$ value being ca. 36 $kJ\,mol^{-1}$. This in turn indicates that "Bzl-passing" is slower and thus has a higher barrier than "Ph-passing." The energy barrier to the GR process in **8** is ca. 10 $kJ\,mol^{-1}$ lower than that in **6**, presumably reflecting the larger steric congestion of the ground state in **8**.

Under the conditions where the Ph-passing process (GR) is fast and the Bzl-passing is slow on the NMR timescale, one of the three *o*-benzeno groups of the Tp moiety should be magnetically nonequivalent to the other two. This situation is not clearly detected in the ^{1}H spectrum (e.g. Fig. 4), but is observed in the ^{13}C spectrum, typically in the lineshape change of the quaternary carbons of the Tp moiety as shown in Fig. 5. At -105 °C, six peaks are observed for the quaternary Tp carbons, indicating the nonequivalence of the three *o*-benzeno groups, though the peaks are not separately assigned. When one raises the temperature, two pairs of peaks broaden and coalesce below ca. -80 °C, leaving the third pair rather sharp. With further increase of the temperature, this pair of peaks broaden and coalesce with the other signals around -60 °C, reflecting the acceleration of the Bzl-passing process, though the rate constants and thus the kinetic parameters for this process could not be determined. At 23 °C two sharp peaks are observed for the quaternary Tp carbons, indicating that both GR and Bzl-passing take place very fast on the NMR timescale at this temperature.

It is interesting that rotation of the benzylic phenyl group is also restricted at low temperatures, because the rotational barrier of the Ph–C bond in a simple benzyl group might be very low: Free energy barriers of below 26 $kJ\,mol^{-1}$ have been reported for dibenzylamine and tribenzylamine.[11]

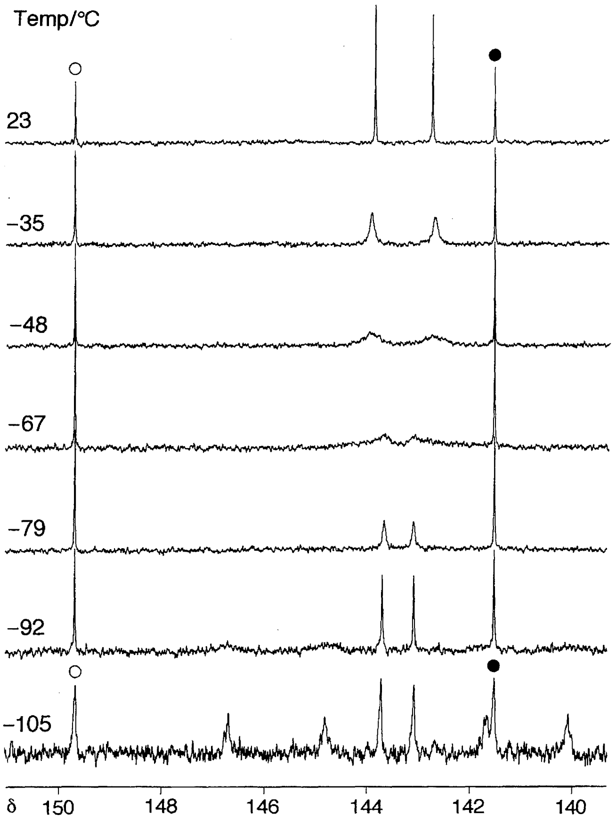

Fig. 5. NMR spectra due to the quaternary Tp carbons of **8** in CD_2Cl_2 at various temperatures. The peaks with ○ and ● are due to the ipso carbons of the *N*-phenyl and *C*-phenyl groups, respectively.

Contrary to *N*-phenyl-9-triptycylamine (**6**) and its *N*-alkyl derivatives **7** and **8**, *N*-2-biphenylyl-9-triptycylamine (**9**) affords ^{1}H and ^{13}C spectra which indicate restricted dynamic processes at 23 °C. The presence of two kinds of *o*-benzeno groups in a 2 : 1 ratio indicates a conformation where the biphenylyl group is frozen in a notch between two *o*-benzeno groups, as shown by the X-ray structure in Fig. 1, and the nitrogen is "planar" on the NMR time scale. Upon raising the temperature one finds that the passing of the biphenylyl group over an *o*-benzeno group becomes fast, as shown by the coalescence of the signals due to the aromatic carbons of the Tp moiety; the lineshape change of 4/5/16 carbon signals in $CDCl_3$ is shown in Fig. 6. Lineshape analysis in the temperature range of 30 to 59 °C together with the saturation transfer experiments at 2 and 12 °C affords rate constants for the rate process, which then give the following kinetic parameters: $\Delta H^{\ddagger} = 65.8 \pm 0.7$ $kJ\,mol^{-1}$, $\Delta S^{\ddagger} = -14.6 \pm 2.4$ $J\,mol^{-1}\,K^{-1}$, $\Delta G^{\ddagger}$ (300 K) $= 70.2$ $kJ\,mol^{-1}$. The gear rotational process may be most plausible for the mechanism; a similar stereodynamic situation was previously discussed for 9-(2-methylbenzyl)triptycene and 9-(2-methylphenoxy)-triptycene.[12] The far higher barrier to GR in **9** than those in **6**—**8** would be ascribed to the presence of the bulkyl phenyl

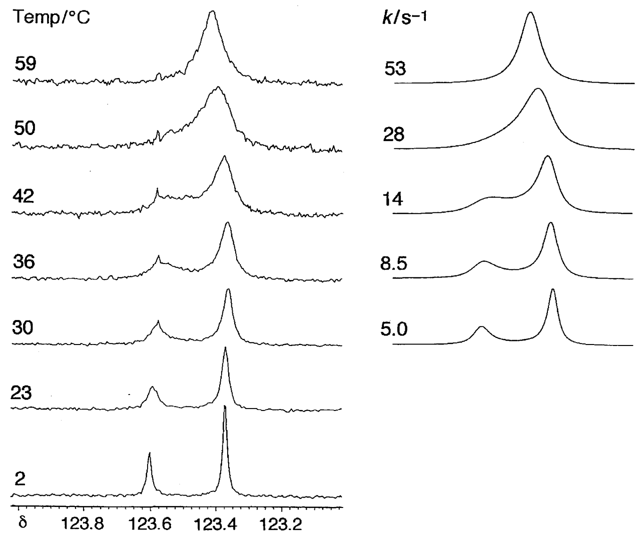

Fig. 6. NMR spectra due to the 4/5/16 carbons of **9** in $CDCl_3$ at various temperatures (left) and the calculated spectra with best-fit rate constants (right).

group in the *o*-position of the *N*-phenyl group in **9**; the GR process in **9** requires the severe steric interaction between the *o*-phenyl group and the Tp skeleton.

In conclusion, dynamic processes in *N*-phenyl-9-triptycylamine (**6**) and *N*-benzyl-*N*-phenyl-9-triptycylamine (**8**) are detected by low-temperature NMR and are reasonably analyzed in terms of the passing of the *N*-substituent(s) over *o*-benzeno groups of the Tp moiety and/or the "isolated rotation" of the *N*-phenyl group. NMR lineshape changes in *N*-2-biphenylyl-9-triptycylamine (**9**) observed above ambient temperature are best interpreted in terms of the passing of the 2-biphenylyl group over *o*-benzeno groups by gear rotation.

Experimental

General. Melting points are not corrected. ^{1}H and ^{13}C NMR spectra were obtained either on a Bruker ARX-300 spectrometer operating at 300.1 MHz for ^{1}H and 75.4 MHz for ^{13}C, respectively, or on a Bruker AM-500 spectrometer operating at 500.2 MHz for ^{1}H and 125.8 MHz for ^{13}C, respectively. Chemical shifts are referenced with internal tetramethylsilane ($\delta_H = 0$) or $CDCl_3$ ($\delta_C = 77.0$). ^{1}H chemical shifts were assigned on the basis of homonuclear double resonance and nuclear Overhauser effect (NOE) experiments. In the ^{13}C data given below, the letters p, s, t, and q denote primary, secondary, tertiary, and quaternary, respectively. ^{13}C chemical shift assignments, when given, were made by ^{13}C–^{1}H COSY experiments. Numberings are as shown in Scheme 4. In variable-temperature experiments, temperatures were calibrated using a methanol or an ethylene glycol sample and are reliable to ±1°C.

***N*-Phenyl-9-triptycylamine (6).** An ice-cooled suspension in 10 mL of chloroform of benzenediazonium-2-carboxylate,[13] prepared from 1.37 g (10 mmol) of anthranilic acid, was added in ca. 1 mL portions at an interval of ca. 1 min to a boiling solution of 1.62 g (6 mmol) of 9-triptycylamine[14] in 30 mL of chloroform, and the mixture was heated under reflux for 30 min. Column chromatography of the reaction mixture through alumina with dichloromethane–hexane as the eluent afforded 954 mg (46%) of *N*-phenyl-9-triptycylamine (**6**) as colorless prisms, mp 280—281 °C. Found: C, 90.12; H, 5.74; N, 3.96%. Calcd for $C_{26}H_{19}N$: C, 90.40; H, 5.54; N, 4.06%. ^{1}H NMR ($CDCl_3$) $\delta = 5.423$ (1H, s, 10-H), 5.513 (1H, br s, NH), 6.754 (2H, br d, $J = 7.6$ Hz, *o*-H), 6.793 (1H, t, $J = 7.3$ Hz, *p*-H), 6.958 (3H, td, $J = 7.5$ and 1.0 Hz, 2/7/14-H), 7.011 (3H, td, $J = 7.1$ and 1.0 Hz, 3/6/15-H), 7.158 (2H, t, $J = 7.7$ Hz, *m*-H), 7.328 (3H, d, $J = 7.4$ Hz, 1/8/13-H), 7.418 (3H, d, $J = 7.3$ Hz, 4/5/16-H). ^{13}C NMR ($CDCl_3$) $\delta = 53.72$ (1C, t, 10-C), 66.69 (1C, q, 9-C), 116.67 (2C, t, *o*-C), 117.87 (1C, t, *p*-C), 122.24 (3C, t, 1/8/13-C), 123.50 (3C, t, 4/5/16-C), 124.58 (3C, t, 2/7/14-C), 125.37 (3C, t, 3/6/15-C), 128.49 (2C, t, *m*-C), 143.58 (3C, q, 8a/9a/12-C), 145.02 (3C, q, 4a/10a/11-C), 145.16 (1C, q, *i*-C).

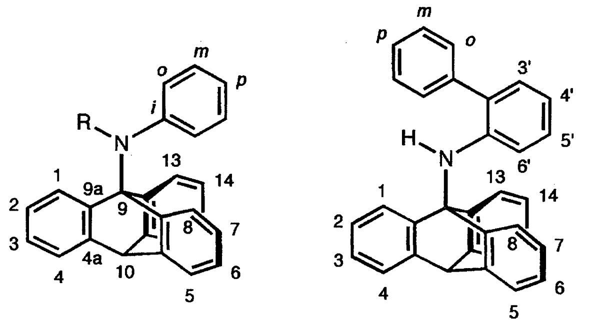

Scheme 4.

***N*-2-Biphenylyl-9-triptycylamine (9).** (a) A similar reaction of 9-triptycylamine as above using a large excess amount (7 molar amount) of benzenediazonium-2-carboxylate, followed by column chromatography through alumina, afforded compound **9** in 35% yield without detection of compound **6** at all. Recrystallization from dichloromethane–hexane afforded crystals containing an equimolar amount of dichloromethane, mp 144—146 °C. Found: C, 78.51; H, 5.05; N, 2.79%. Calcd for $C_{32}H_{23}N \cdot CH_2Cl_2$: C, 78.26; H, 4.98; N, 2.77%. ^{1}H NMR ($CDCl_3$) $\delta = 5.398$ (1H, s, 10-H), 5.823 (1H, br s, NH), 6.413 (1H, d, $J = 8.2$ Hz, 6′-H), 6.740 (1H, br d, $J = 7.0$ Hz, 1-H), 6.84—7.06 (8H, m), 7.29—7.35 (4H, m, 8/13-H, 4-H, and 3′-H), 7.431 (2H, d, $J = 7.0$ Hz, 5/16-H), 7.499 (1H, t, $J = 7.3$ Hz, *p*-H), 7.611 (2H, t, $J = 7.8$ Hz, *m*-H), 7.797 (2H, d, $J = 7.3$ Hz, *o*-H). ^{13}C NMR ($CDCl_3$) $\delta = 53.69$ (1C, t, 10-C), 66.81 (1C, q, 9-C), 117.33 (1C, t, 6′-C), 117.57 (1C, t, 4′-C), 117.87 (1C, t, 1-C), 123.37 (2C, t, 5/16-C), 123.60 (1C, t, 4-C), 124.43 (2C, t, 8/13-C), 124.45 (2C, t, 7/14-C), 124.83 (1C, t, 2-C), 125.04 (1C, t, 3-C), 125.47 (2C, t, 6/15-C), 127.37 (1C, t, 5′-C), 127.76 (1C, t, *p*-C), 128.19 (1C, q, 2′-C), 129.24 (2C, t, *m*-C), 129.69 (2C, t, *o*-C), 130.04 (1C, t, 3′-C), 139.71 (1C, q), 141.88 (1C, q), 142.62 (2C, q), 144.39 (2C, q), 145.46 (1C, q), 146.11 (1C, q).

(b) Reaction of *N*-phenyl-9-triptycylamine (**6**) with 2 molar amounts of benzenediazonium-2-carboxylate also afforded **9** in 78% yield.

***N*-Methyl-*N*-phenyl-9-triptycylamine (7).** To a chilled (−70 °C) solution of 270 mg (0.78 mmol) of *N*-phenyl-9-triptycylamine (**6**) in 3 mL of dry tetrahydrofuran (THF) under Ar was added 0.85 mL (1.36 mmol) of butyllithium in hexane (10 w/v%) and the mixture was stirred for 0.5 h at −50 °C. To this solution was added 0.5 mL (8.0 mmol) of methyl iodide and the mixture was left to warm up to room temperature with stirring. The reaction mixture was poured into water and extracted with dichloromethane. The organic layer was washed with brine twice and dried over anhydrous sodium sulfate. After evaporation of the solvent, the residue was chromatographed on alumina with hexane–benzene as the eluent. Recrystallization of the eluted product from dichloromethane–hexane afforded 250 mg (89%) of compound **7**, mp 210—211 °C. Found: C, 90.51; H, 5.86; N, 3.89%. Calcd for $C_{27}H_{21}N$: C, 90.21; H, 5.89; N, 3.90%. ^{1}H NMR ($CDCl_3$) $\delta = 3.852$ (3H, s,

CH_3), 5.334 (1H, s, 10-H), 6.862 (1H, t, $J=7.3$ Hz, *p*-H), 6.899 (3H, td, $J=7.6$ and 1.2 Hz, 2/7/14-H), 6.914 (2H, td, $J=8.0$ and 1.0 Hz, *o*-H), 6.972 (3H, td, $J=7.3$ and 1.0 Hz, 3/6/15-H), 7.120 (2H, dd, $J=$ 8.5 and 7.3 Hz, *m*-H), 7.320 (3H, d, $J=7.6$ Hz, 1/8/13-H), 7.387 (3H, d, $J=7.2$ Hz, 4/5/16-H). ^{13}C NMR ($CDCl_3$) δ = 46.73 (1C, p, CH_3), 54.48 (1C, t, 10-C), 75.47 (1C, q, 9-C), 119.78 (1C, t, *p*-C), 122.19 (2C, t, *o*-C), 123.33 (3C, t, 4/5/16-C), 124.12 (3C, t, 2/7/14-C), 124.97 (3C, t, 3/6/15-C), 125.17 (3C, t, 1/8/13-C), 127.38 (2C, t, *m*-C), 144.11 (3C, q, 4a/10a/11-C), 145.53 (3C, q, 8a/9a/12-C), 152.17 (1C, q, *i*-C).

***N*-Benzyl-*N*-phenyl-9-triptycylamine (8).** To a solution of 200 mg (0.58 mmol) of *N*-phenyl-9-triptycylamine (**6**) in 3 mL of dry THF at −75 °C was added 0.73 mL (1.16 mmol) of butyllithium in hexane (1.6 mol dm^{-3}), and the mixture was stirred at −70 °C for 30 min under Ar atmosphere. To the solution was added 1.38 mL (11.6 mmol) of benzyl bromide at −60 °C. The mixture was stirred for 3 h, poured into water, and extracted with dichloromethane (50 mL×4). The combined extracts were washed with brine and dried over anhydrous sodium sulfate. After evaporation of the solvent, the residue was chromatographed through alumina with hexane as the eluent. The eluted product was recrystallized from benzene–hexane to afford 45 mg (18%) of compound **8** as colorless crystals containing one molar amount of benzene. Found: C, 91.44; H, 6.29; N, 2.71%. Calcd for $C_{33}H_{25}N\cdot C_6H_6$; C, 91.19; H, 6.08; N, 2.73%. ^{1}H NMR ($CDCl_3$) $\delta=5.362$ (1H, s, 10-H), 5.429 (2H, s, CH_2), 6.637 (2H, d, $J=8.2$ Hz, *o*-H), 6.756 (1H, t, $J=7.3$ Hz, *p*-H), 6.812 (3H, td, $J=7.6$ and 1.2 Hz, 2/7/14-H), 6.934 (2H, dd, $J=8.5$ and 7.3 Hz, *m*-H), 6.968 (3H, td, $J=7.3$ and 0.8 Hz, 3/6/15-H), 7.351 (3H, d, $J=7.0$ Hz, 1/8/13-H), 7.396 (1H, t, $J=7.0$ Hz, *p*′-H), 7.405 (3H, d, $J=7.3$ Hz, 4/5/16-H), 7.526 (2H, t, $J=7.6$ Hz, *m*′-H), 7.793 (2H, d, $J=7.3$ Hz, *o*′-H). ^{13}C NMR ($CDCl_3$) $\delta=54.63$ (1C, t, 10-C), 60.76 (1C, s, CH_2), 76.24 (1C, q, 9-C), 119.25 (1C, t, *p*-C), 120.55 (2C, t, *o*-C), 123.49 (3C, t, 4/5/16-C), 124.29 (3C, t, 2/7/14-C), 125.04 (3C, t, 1/8/13-C), 125.14 (3C, t, 3/6/15-C), 126.68 (2C, t, *o*′-C), 126.84 (1C, t, *p*′-C), 127.04 (2C, t, *m*-C), 128.96 (2C, t, *m*′-C), 142.84 (1C, q, *i*′-C), 143.93 (3C, q, 4a/10a/11-C or 9a/8a/12-C), 145.01 (3C, q, 4a/10a/11-C or 9a/8a/12-C), 150.94 (1C, q, *i*-C).

Table 2. Crystal Data of Compound **9** and Parameters for Data Collection, Structure Determination and Refinement

Empirical formula	$C_{32}H_{23}N\cdot CH_2Cl_2$
Formula weight	506.48
Crystal dimension/mm	0.3 × 0.5 × 0.8
Crystal system	Monoclinic
Space group	$P2_1/c$ (#4)
a/Å	8.968(2)
b/Å	11.128(2)
c/Å	26.424(2)
β/°	97.43(1)
V/Å^3	2615.0(7)
Z	4
D_c/g cm^{-3}	1.286
F(000)	1056.00
μ(Mo $K\alpha$) /cm^{-1}	2.70
Temp/°C	22 ± 1
Scan width/°	$0.68\pm0.30\tan\theta$
$2\theta_{max}$/°	54.9
No. of reflections measured	
Total	5191
Unique	4863
No. of refinement variables	397
Final R; R_w	0.058; 0.037

Lineshape Analysis. Total lineshape analysis was performed by visual matching of experimental spectra with theoretical spectra with theoretical spectra computed on an NEC PC9821Xs personal computer equipped with a Mutoh PP-210 plotter using the DNMR3K program, a modified version of the DNMR3 program[15] converted for use on personal computers by Dr. H. Kihara of Hyogo University of Teacher Education. Temperature dependences of chemical shift differences and T_2 values were properly taken into account.

Saturation Transfer Experiments.[16] In the analysis of the rate process in compound **9**, the 5/16-H signal at $\delta=7.33$ was irradiated and the change in the intensity of the 4-H signal at $\delta=6.75$ was observed. Rate constants were obtained by nonlinear least-squares analysis of the data: 0.32 and 0.92 s^{-1} at 2 and 12 °C, respectively.

X-Ray Crystallography. Crystals of compound **9** were grown from dichloromethane–hexane and contained one equivalent of dichloroethane. The crystal data and the parameters for data collection, structure determination and refinement are summarized in Table 2. Diffraction data were collected on a Rigaku AFC7R diffractometer and calculations were performed using the teXsan program.[17] The structure was solved by direct methods, followed by full-matrix least-squares refinement with all non-hydrogen atoms anisotropic and hydrogen atoms isotropic. Reflection data with $|F_o|>3\sigma(F_o)$ were used. The function minimized was $\sum\omega(|F_o|-|F_c|)^2$ where $\omega=[\sigma^2(F_o)]^{-1}$.

References

1) D. Gust and K. Mislow, *J. Am. Chem. Soc.*, **98**, 1535 (1973); K. Mislow, *Acc. Chem. Res.*, **9**, 26 (1976).

2) H. Iwamura and K. Mislow, *Acc. Chem. Res.*, **21**, 175 (1988).

3) G. Yamamoto, *Pure Appl. Chem.*, **92**, 569 (1990).

4) G. Yamamoto, *Tetrahedron*, **79**, 2761 (1990).

5) A preliminary report has been published: G. Yamamoto, H. Higuchi, M. Yonebayashi, Y. Nabeta, and J. Ojima, *Chem. Lett.*, **1995**, 853.

6) G. Yamamoto, H. Higuchi, M. Yonebayashi, and J. Ojima, *Chem. Lett.*, **1994**, 1911; G. Yamamoto, H. Higuchi, M. Yonebayashi, Y. Nabeta, and J. Ojima, *Tetrahedron*, **52**, 12409 (1996).

7) See for example: J. C. Evans, *Spectrochim. Acta*, **16**, 428 (1960); D. G. Lister and J. K. Tyler, *J. Chem. Soc., Chem. Commun.*, **1966**, 152; F. A. L. Anet and M. Ghiaci, *J. Am. Chem. Soc.*, **101**, 6857 (1979).

8) We recently found that in *N*-alkyl-*N*-9-triptycylacetamides where the alkyl is methyl or ethyl, the amide nitrogen atom is significantly pyramidalized both in crystal and in solution: G. Yamamoto, H. Murakami, N. Tsubai, and Y. Mazaki, *Chem. Lett.*, **1997**, 605; G. Yamamoto, N. Tsubai, H. Murakami, and Y. Mazaki, *Chem. Lett.*, **1997**, 1295.

9) G. Yamamoto and M. Ōki, *Bull. Chem. Soc. Jpn.*, **54**, 473 (1981).

10) See for example: M. Ōki, "Applications of Dynamic NMR Spectroscopy to Organic Chemistry," VCH Publishers, Deerfield Beach (1985), p. 5.

11) S. H. Fleischman, M. R. Whalon, C. D. Rithner, G. L. Grady, and C. H. Bushweller, *Tetrahedron Lett.*, **23**, 4233 (1982).

12) G. Yamamoto, T. Nemoto, and Y. Ohashi, *Bull. Chem. Soc. Jpn.*, **65**, 1957 (1992).

13) F. M. Logullo, A. H. Seitz, and L. Friedman, *Org. Synth.*,

Coll. Vol. V, 54 (1973).

14) W. Theilacker and K.-H. Beyer, *Chem. Ber.*, **97**, 2968 (1961).

15) D. A. Kleier and G. Binsch, QCPE Program No. 165.

16) S. Forsén and R. A. Hofmann, *J. Chem. Phys.*, **39**, 2892 (1963); J. Sandström, "Dynamic NMR Spectroscopy," Academic Press, London (1982), Chap. 4; G. Yamamoto, *Bull. Chem. Soc. Jpn.*, **65**, 1967 (1992).

17) "teXsan: Crystal Structure Analysis Package," Molecular Structure Corporation (1985 and 1992).